

Regulating the ARNT/TACC3 Axis: Multiple Approaches to Manipulating Protein/Protein Interactions with Small Molecules

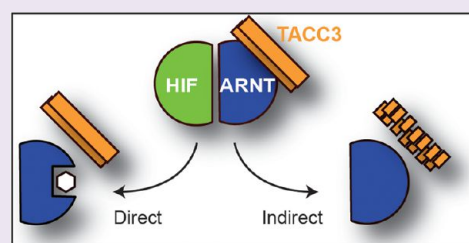
Yirui Guo,^{†,‡} Carrie L. Partch,^{†,‡,||} Jason Key,^{†,‡} Paul B. Card,^{†,‡} Victor Pashkov,[‡] Anjana Patel,[§] Richard K. Bruick,[‡] Heiko Wurdak,[§] and Kevin H. Gardner^{*,†,‡}

[†]Departments of Biophysics and [‡]Biochemistry, UT Southwestern Medical Center, 5323 Harry Hines Boulevard, Dallas, Texas 75390-8816, United States

[§]Leeds Institute of Molecular Medicine, University of Leeds, St. James's University Hospital, Beckett Street, Leeds LS9 7TF, U.K.

S Supporting Information

ABSTRACT: For several well-documented reasons, it has been challenging to develop artificial small molecule inhibitors of protein/protein complexes. Such reagents are of particular interest for transcription factor complexes given links between their misregulation and disease. Here we report parallel approaches to identify regulators of a hypoxia signaling transcription factor complex, involving the ARNT subunit of the HIF (Hypoxia Inducible Factor) activator and the TACC3 (Transforming Acidic Coiled Coil Containing Protein 3) coactivator. In one route, we used *in vitro* NMR and biochemical screening to identify small molecules that selectively bind within the ARNT PAS (Per-ARNT-Sim) domain that recruits TACC3, identifying KG-548 as an ARNT/TACC3 disruptor. A parallel, cell-based screening approach previously implicated the small molecule KHS101 as an inhibitor of TACC3 signaling. Here, we show that KHS101 works indirectly on HIF complex formation by destabilizing both TACC3 and the HIF component HIF-1 α . Overall, our data identify small molecule regulators for this important complex and highlight the utility of pursuing parallel strategies to develop protein/protein inhibitors.



While many small molecule enzyme inhibitors and receptor ligands that modulate cellular signaling pathways have been discovered for research and therapeutic use, comparable reagents that target non-enzymatic protein/protein interactions are relatively rare. While such compounds are available for several systems, technical issues, from the suitability of compounds in screening libraries to the difficulty of predicting “druggable” sites,^{1,2} complicate the development of specific inhibitors of targeted protein/protein interactions.

Such inhibitors have been particularly sought for transcription factors and their associated regulatory proteins,^{1,3} given well-validated links between misregulation of these proteins and disease. Here we focus on one such complex as a model: hypoxia inducible factor (HIF), the central regulator of the mammalian hypoxia response.⁴ HIF is a heterodimer of two bHLH-PAS (basic Helix Loop Helix-Per-ARNT-Sim) subunits, including a HIF- α paralog (HIF-1 α , -2 α , -3 α) and aryl hydrocarbon receptor nuclear translocator (ARNT, also known as HIF- β) (Figure 1a). While O₂-dependent post-translational hydroxylation normally lowers both HIF- α abundance and activity, these modifications are reduced under hypoxia and allow HIF- α to accumulate in the nucleus.⁵ Subsequently, HIF complexes form and control the expression of several hundred genes, including potent angiogenic and growth factors.⁶ As such, abnormally high levels of HIF correlate with several forms of cancer, suggesting that HIF inhibitors could potentially block tumor formation and progression.⁵ Such inhibition might be achieved by blocking

the HIF- α and ARNT interaction, which uses interchain contacts between bHLH and PAS (Per-ARNT-Sim) domains.^{7–11} While we have successfully found inhibitors that use this approach by exploiting a ligand-binding cavity within one of the HIF-2 PAS domains,^{9,10} differences among HIF- α sequences suggest that this route is paralog-specific.

To simultaneously inhibit all HIF complexes, we considered targeting interactions between the ARNT subunit, shared among these complexes, with transcriptional coactivators. This strategy is predicated on the ARNT PAS-B domain (Figure 1) directly recruiting coiled coil coactivators (CCCs) to HIF for proper transcriptional regulation.^{12–14} By depleting endogenous proteins or overexpressing mutants, we found that HIF complexes differentially utilize several CCC proteins including thyroid hormone receptor interacting protein 230 (TRIP230¹⁵), coiled-coil coactivator (CoCoA¹⁶), and transforming acidic coiled-coil 3 (TACC3¹⁷) at different promoters.¹⁴ Combining biophysical and mutagenesis data, we generated a structural model of the ARNT/TACC3 complex, showing that CCC proteins use a coiled coil to bind a helical surface on ARNT PAS-B (Figure 1b).^{12,14} Notably, the CCC-binding surface on ARNT is near where other PAS domains bind cofactors that modulate their protein/protein interactions,¹⁸ leading us to hypothesize that artificial ARNT-binding

Received: July 23, 2012

Accepted: December 14, 2012

Published: December 14, 2012

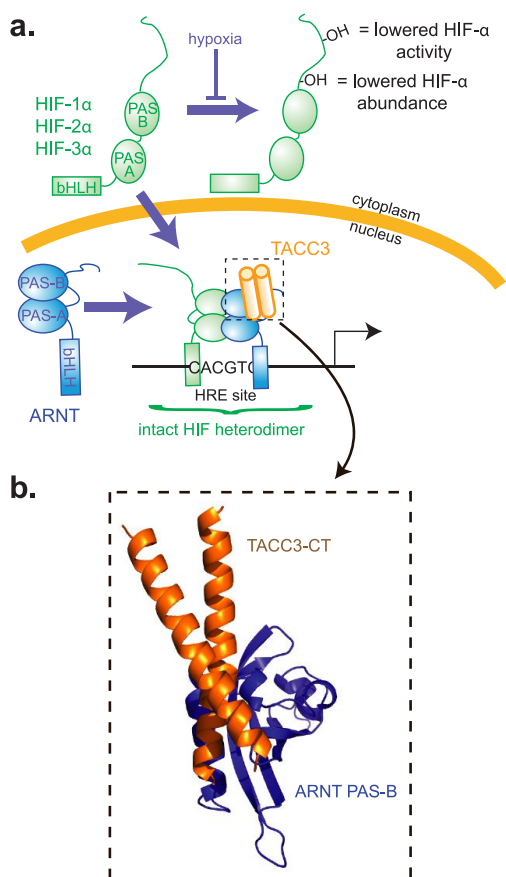


Figure 1. Overview of the ARNT/TACC3 complex. (a) Schematic of HIF complexes, which are bHLH-PAS heterodimers that include an O_2 -sensitive HIF- α subunit and a constitutive ARNT subunit. Under normoxia, O_2 -dependent hydroxylation of HIF- α decreases its abundance and activity.⁵ Hypoxia stops these modifications, allowing HIF- α to accumulate in the nucleus and dimerize with ARNT. This heterodimer binds to hypoxia responsive enhancer (HRE) sites, controlling target gene transcription. In addition to binding HIF- α , ARNT PAS-B directly recruits CCC proteins.^{12,14} (b) Structural model of an ARNT/CCC complex¹⁴ showing how the TACC3 coiled coil interacts with the helical surface of ARNT PAS-B, opposite from where HIF- α PAS-B binds.

compounds might similarly control ARNT PAS-B/CCC interactions to regulate HIF activity.

Here we characterize the mechanisms of action of two small molecule inhibitors of ARNT/TACC3 signaling, identified from independent *in vitro* target-based and cell-based phenotypic screens. The first approach took advantage of our NMR studies of ARNT PAS-B,¹⁹ letting us use this method to screen over 760 compounds^{20,21} for protein binding. One ARNT-binding compound, KG-548, binds in a cavity adjacent to the TACC3 binding site and displaces CCCs from ARNT *in vitro*. In parallel, we investigated KHS101, a thiazole derivative originally identified in a cell-based phenotypic screen²² that specifically induces neuronal differentiation.²³ Based on KHS101 affecting aspects of the neuronally expressed ARNT homologue, ARNT2, in neural progenitor cells (NPCs) and cross-linking to TACC3 in NPC lysates, the question arises as to whether KHS101 directly disrupts the ARNT2/TACC3 interaction. We show that KHS101 does not directly bind to the minimal ARNT or TACC3 interacting domains but instead promotes TACC3 protein turnover within cells, indicating an

indirect mode of function. Notably, KHS101 also promotes the turnover of the HIF-1 α subunit itself and interferes with HIF-driven transcription in living cells under hypoxia, as anticipated by these effects on the levels of both activator (HIF-1 α) and coactivator (TACC3) components. Taken together, KG-548 and KHS101 provide useful molecules for studies of HIF signaling and, more broadly, valuable examples of different ways to control protein complex formation with small molecules.

RESULTS

Identifying Direct Inhibitors of ARNT/TACC3 Interactions by NMR Screening. We have solved a new 1.6 Å resolution X-ray diffraction structure of ARNT PAS-B (Table 1;

Table 1. X-ray Crystallography Data Processing and Refinement Statistics

	Data Collection	
space group		C2
cell dimensions		
<i>a</i> , <i>b</i> , <i>c</i> (Å)		93.3, 61.7, 55.5
β (deg)		124.6
resolution (Å)		20.7 to 1.6 (1.63 to 1.60)
R_{sym} or R_{merge}		4.7 (43.9)
I/σ_1		38.8 (2.2)
observed reflections		155,415
unique reflections		34402
completeness % (highest shell)		99.9 (100)
	Refinement	
resolution (Å)		22.5 to 1.6 (1.63 to 1.60)
$R_{\text{work}}/R_{\text{free}}$		20.15/22.65
no. atoms		
protein		1832
water		206
av <i>B</i> -factor		
protein		20.3
water		35.4
R.M.S. deviations		
bond lengths (Å)		0.014
bond angles (deg)		1.45

Figure 2a), revealing two cavities near the regulatory cofactor binding sites in other PAS domains (e.g., flavins in photosensors; heme in oxygen sensors^{24,25}). The larger 65 Å³ cavity is flanked by the E α /F α helices, G β /H β /I β strands and the AB loop, and includes several polar residues (e.g., S411, T441, and S443) that facilitate the binding of three waters at typical cofactor sites. A hydrophobic side of the cavity, involving V397, L408, F412, and F427, is shared with the CCC-binding surface in our ARNT/TACC3 model.¹⁴ The second cavity is slightly smaller (40 Å³) and comparable to the chromophore binding site in photoactive yellow protein.²⁶ While these cavities are relatively small, their locations (and potential for merge into a single larger cavity) raised the potential for them to bind artificial compounds and modulate CCC binding, similarly to other PAS domains.

To identify such compounds, we used solution NMR to search over 760 small molecules^{9,20,21} for ARNT PAS-B binding. This library consists of low molecular weight fragments (average MW: 203 ± 73 Da, Supplementary Table S1) containing “privileged” moieties enriched in protein-

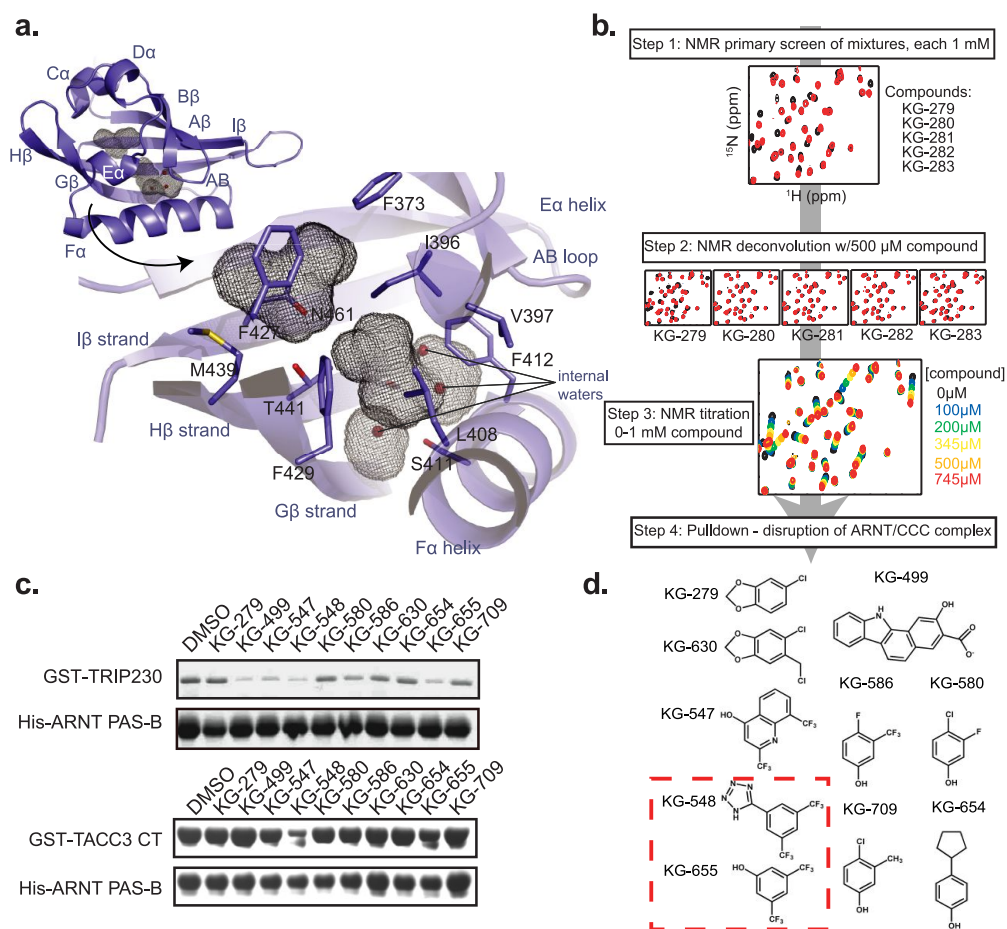


Figure 2. Screening ARNT PAS-B for small molecule effectors of the ARNT/TACC3 interaction. (a) Diagram of the ARNT PAS-B crystal structure, shown inset with secondary structure designations and internal cavities (gray mesh). The larger cavity is adjacent to the TACC3 binding site and contains three waters; the smaller cavity is primarily hydrophobic. (b) Schematic of the NMR-based screen for compounds that bind ARNT PAS-B. Initial $^{15}\text{N}/^1\text{H}$ HSQC spectra were acquired with $250\ \mu\text{M}$ ^{15}N -labeled ARNT PAS-B with a mixture of five compounds (1 mM each); mixtures producing large chemical shift perturbations (compared to DMSO) were deconvoluted as shown. (c) Lead compounds ($500\ \mu\text{M}$ each) from NMR-based screen were tested for their ability to disrupt complexes of ARNT PAS-B with CCC fragments of TRIP230 (1583–1716) and TACC3 (561–631 = TACC3-CT). (d) Summary of ARNT PAS-B binding and ARNT/CCC disruption of tested compounds. All 10 compounds generated chemical shift perturbations when titrated into ARNT PAS-B; KG-548 and KG-655 (red box) also disrupted TRIP230 and TACC3 binding to ARNT PAS-B *in vitro*.

binding compounds.²⁷ Further, this collection has previously provided us several compounds (or analogues) that bind to other PAS domains^{9,10,20} and disruptors of protein/protein interactions in other transcriptional regulators.^{9,21}

We quickly evaluated these compounds for ARNT PAS-B binding using protein-detected NMR (Figure 2b). In the primary screen, $^{15}\text{N}/^1\text{H}$ HSQC spectra were acquired on ^{15}N -labeled ARNT PAS-B samples mixed with five candidate compounds ($250\ \mu\text{M}$ protein, 1 mM each compound) or DMSO. Compound mixtures that produced changes in peak locations or intensities indicated that one or more compounds bound the protein target; 16 such mixtures were subsequently deconvoluted by acquiring spectra on ARNT PAS-B with individual compounds. Eighteen hits from these steps were tested in titrations at concentrations up to 1 mM to establish binding potency and location; 10 of these (Figure 2c) were soluble throughout this concentration range and further studied.

To examine whether these ARNT-binding compounds affected the stability of ARNT PAS-B/CCC complexes, we initially checked their disruption of ARNT-mediated pull-downs

of fragments of the TRIP230 and TACC3 coactivators (Figure 2c). The fragments of both CCC proteins contained the coiled coil that binds ARNT PAS-B,^{12,14} facilitating robust interaction without compounds present. However, several chemicals markedly interfered with ARNT binding to one or both coactivators. Among these, KG-548 exhibited the greatest reduction of ARNT/CCC complex formation for both coactivators, with a smaller effect seen for the structurally related fragment KG-655 (Figure 2d).

KG-548 Binds to the Cavity of ARNT PAS-B. Next, we further characterized compound-mediated ARNT/CCC disruption with solution NMR to identify ligand-binding sites within ARNT PAS-B. Using KG-548 as the most effective disruptor of this complex, we observed slow exchange behavior in compound titrations monitored by ARNT PAS-B $^{15}\text{N}/^1\text{H}$ HSQC spectra (Figure 3a), suggesting micromolar (or tighter) dissociation constants. We used our prior chemical shift assignments¹⁹ to map ligand-induced changes onto the ARNT PAS-B structure using minimum chemical shift difference analyses, assuming correlations between the nearest pairs of peaks in apo- and KG-548 saturated spectra (Figure

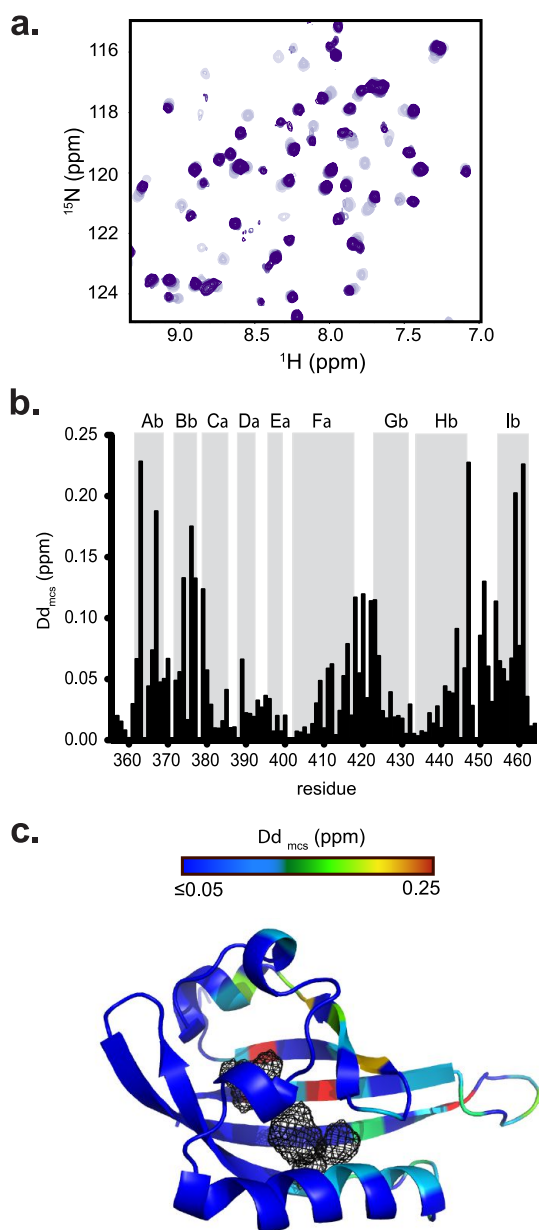


Figure 3. KG-548 appears to bind within the ARNT PAS-B cavities. (a) $^{15}\text{N}/^1\text{H}$ HSQC spectra of a KG-548 titration (0–1 mM from light to dark crosspeaks) into $320\ \mu\text{M}$ ^{15}N ARNT PAS-B. Slow exchange behavior was observed, indicated by the disappearance of apo-crosspeaks and concomitant appearance of new peaks. (b) Minimum chemical shift analysis⁴⁵ of KG-548 titration into ARNT PAS-B, mapped onto the sequence and secondary structure. (c) Chemical shift mapping suggests that KG-548 binds the ARNT PAS-B cavities, as shown by a heat map of KG-548-induced chemical shift changes on the ARNT PAS-B crystal structure ($\Delta\delta_{\text{mcs}}$ colored from low (blue) to high (red)) with the largest changes near the internal cavities (mesh).

3b). Residues that were most strongly affected by KG-548 addition were located close to the internal ARNT PAS-B cavities (Figure 3b,c) and analogous to where other PAS domains often bind ligands.²⁸ Notably, these ligand-mediated structural and functional effects were sensitive to minor changes in compound structure. Two KG-548 variants with small changes, CF_3 to Cl substitutions on the phenyl ring, and addition of methyl or ethyl moieties on the tetrazole, bound ARNT more weakly and were unable to disrupt ARNT/

TACC3 complexes (Supplementary Figure S1a–e). Coupled with the limited number of leads from the library screen, these data demonstrate specificity of the ARNT/ligand interaction.

KG-548 Binding Shows Selectivity among PAS Domain Targets. Having demonstrated specificity from the ligand perspective, we next explored the potential for other bHLH-PAS PAS-B domains to bind KG-548. We started by examining ARNT2, a closely related ARNT homologue that is chiefly expressed in neuronal and kidney tissue^{29,30} (Supplementary Figure S2). Using solution NMR methods, we verified that the ARNT and ARNT2 PAS-B domains adopt comparable structures, as expected from the 80% sequence identity between them. Similarities in chemical shifts and TALOS+-derived secondary structures³¹ (Supplementary Figure S3a,b) strongly indicate ARNT2 adopts the same overall fold as seen in our crystal (Figure 2 and ref 9) and solution¹⁹ structures of ARNT PAS-B, giving us confidence in a ARNT2 PAS-B homology model to suggest the placement of residues involved in ARNT/CCC interactions¹⁴ (Supplementary Figure S3c).

To functionally test these structural similarities, we examined the ability of ARNT2 PAS-B to bind coactivator fragments and KG-548. Pull-down experiments demonstrated that ARNT2 PAS-B directly interacts with GST-tagged TACC3-CT (=C-terminal 70 aa of TACC3, including residues 561–631) *in vitro* (Supplementary Figure S3d), as seen for ARNT (Figure 2c). Mutations to ARNT2 PAS-B residues E372 and K391 weakened this interaction (Supplementary Figure S3d), chosen for their similarity to ARNT E398 and K417 (Supplementary Figure S3c).¹⁴ $^{15}\text{N}/^1\text{H}$ HSQC spectra of both ARNT2 E372A and K391A PAS-B mutants were similar to wildtype protein (Supplementary Figure S3e), suggesting that both point mutations had minimal structural effects. Next, we asked if KG-548 could also bind to ARNT2 PAS-B and compete away TACC3. Ligand titrations monitored with $^{15}\text{N}/^1\text{H}$ HSQC spectra showed the same slow exchange (Supplementary Figure S4a) observed with ARNT PAS-B, with the largest effects (Supplementary Figure S4b,c) clustered in the same internal sites (Supplementary Figure S2). Finally, as expected from the similar CCC and ligand binding modes, KG-548 also disrupts ARNT2 PAS-B/TACC3 interactions in pull-down assays (Supplementary Figure S4d), underscoring the high degree of similarity between ARNT and ARNT2.

In contrast, similar titrations of KG-548 into two more widely diverged PAS-B domains from the BMAL-1 and HIF-2 α bHLH-PAS proteins (38% and 34% identity to ARNT PAS-B) showed specificity in the protein/ligand interaction. We observed very few chemical shift changes caused by KG-548 addition to BMAL-1, and virtually none with HIF-2 α (Supplementary Figure S5) despite large cavities within both PAS domains.^{9,10,32} We interpret these data to indicate that these two PAS-B domains have (much) lower affinities for KG-548 than ARNT PAS-B, showing little to no interaction at the tested concentrations and thus establishing that observed ligand-binding specificity is not solely based on simple accessibility. More broadly, we have not observed KG-548 binding to other PAS and non-PAS targets,^{20,21} consistent with the specificity that can be observed in small fragments from other libraries.³³

KG-548 Breaks up the ARNT/TACC3 Complex *in Vitro* and in Cell Lysate. To further characterize KG-548 induced disruption of ARNT/TACC3, we examined the dose dependence of this effect in two ways. Pull-down assays using His-ARNT PAS-B and GST-TACC3-CT, tagged versions of the

minimal interacting components of both proteins,¹⁴ showed that levels of GST-TACC3-CT pulled down by His-ARNT PAS-B decreased in a KG-548 dose-dependent manner (Figure 4a) at concentrations that perturbed ARNT PAS-B NMR

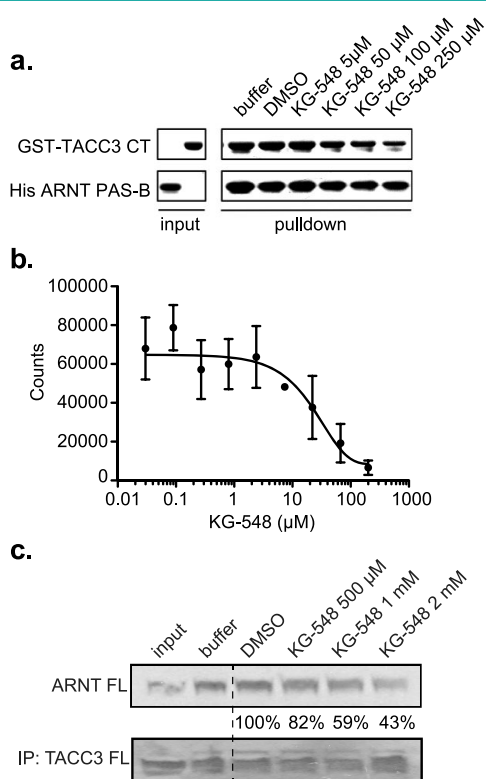


Figure 4. KG-548 disrupts *in vitro* ARNT/TACC3 interactions. (a) Titration of KG-548 into an *in vitro* pull-down assay of minimal ARNT PAS-B and TACC3-CT interacting fragments shows a dose-dependent reduction in ARNT/TACC3 complex formation. (b) Quantification of KG-548 potency for disrupting the ARNT PAS-B/TACC3-CT interaction as provided by AlphaScreen, showing an apparent IC_{50} of 25 μ M. (c) Co-immunoprecipitation assays of full length ARNT and TACC3 proteins in HEK293T cell lysates show that KG-548 weakens the ARNT/TACC3 interaction as demonstrated by the dose-dependent decrease in the intensity of the ARNT protein band (quantitated with % remaining compared to DMSO control) associated with immunoprecipitated TACC3 protein.

spectra. We quantified the potency of KG-548 using AlphaScreen, a luminescence proximity assay of complex formation between the two tagged fragments (Supplementary Figure S6a). The assay was validated by showing that untagged ARNT PAS-B or TACC3 competed against complex formation between tagged proteins with IC_{50} of \sim 2–3 μ M (Supplementary Figure S6b). Similar AlphaScreen assays with KG-548 showed a 25 μ M IC_{50} inhibition (Figure 4b), consistent with the apparent ARNT PAS-B/KG-548 affinity seen in NMR-based titrations.

To examine how well these results from isolated domains translate to full length proteins, we surveyed the ability of KG-548 to disrupt the complex between full length human ARNT and mouse TACC3 proteins. While cell-based qPCR and HRE reporter assays of this effect were hampered by issues with cell toxicity at midmicromolar KG-548 concentrations, an alternative was provided by immunoprecipitation experiments in lysates of HEK 293T cells transfected with expression vectors for both proteins. Within this system, the ARNT/TACC3

interaction can clearly be observed by co-IP without ligand present; addition of increasing concentrations of KG-548 leads to a progressive decrease in the amount of TACC3-associated ARNT protein (Figure 4c). While the apparent potency of KG-548 is lower in this more complex setting, our data clearly demonstrate that this ARNT-binding compound can inhibit ARNT/TACC3 complex formation in truncated or full length proteins. Notably, two negative control compounds, KG2-006 and KG2-007, did not show such inhibition at comparable concentrations, consistent with the isolated domain results (Supplementary Figure S1f).

Discovery of KHS101 as a TACC3 Inhibitor. Complementing our targeted *in vitro* screening, we examined a presumed disruptor of ARNT/CCC interactions provided by the HTS-derived compound KHS101 (Supplementary Figure S7a) that accelerates NPC differentiation in the adult rat.²³ Cross-linking data initially associated TACC3 with KHS101 by showing that a benzophenone derivative bound TACC3 at an uncharacterized location. This linkage between KHS101 and TACC3 was underscored by the observation of similar cellular effects with either KHS101 treatment or anti-TACC3 siRNAs in several settings,^{23,34} suggesting that this compound is a general TACC3 inhibitor. However, this study did not characterize the mechanism of KHS101 action on TACC3, leading us to ask if KHS101 (1) directly interferes with TACC3 binding to its partners ARNT or ARNT2 PAS-B *in vitro*, (2) alters TACC3 protein levels in cells, or (3) affects transcription from ARNT/CCC-reliant promoters, such as HIF-driven genes.¹⁴

KHS101 Is Not a Direct Regulator of the ARNT/TACC3 Complex. To address how KHS101 regulates ARNT/TACC3, we performed *in vitro* pull-down experiments in the presence of KHS101 using the minimal constructs of both proteins. We did not observe any substantial KHS101-dependent effect on TACC3 pull-downs with either ARNT or ARNT2 (Supplementary Figure S7b,c), suggesting that KHS101, in contrast to KG-548, works indirectly to disrupt ARNT/TACC3 function. To test this hypothesis, we used solution NMR spectroscopy to examine KHS101 binding to ARNT PAS-B and TACC3. $^{15}N/^1H$ HSQC spectra of ARNT PAS-B titrated with KHS101 showed only minor changes (Supplementary Figure S7d; compare to Figure 3a for KG-548), indicating no binding. Analogous spectra using a ^{15}N -labeled minimal version of TACC3 with both the ARNT-interacting C-terminal 21 residues of TACC3 and a stabilizing GCN4 coiled coil (GCN4-TACC3-min) also showed no differences between DMSO and KHS101-treated samples (Supplementary Figure S7e) at concentrations that trigger biological responses (*vide infra* and ref 23). These negative data strongly suggested that KHS101 perturbs the ARNT/TACC3 complex in a different, likely indirect, mechanism than KG-548.

KHS101 Reduces Intracellular TACC3 Stability. Coupling prior data implicating KHS101 interference with ARNT/TACC3²³ with our observation that KHS101 does not directly block the minimal ARNT PAS-B/TACC3-CT interaction, we hypothesized that KHS101 might function indirectly by modulating TACC3 stability. To test this, we examined TACC3 protein stability in HEK293T cells using pulse chase experiments conducted with the translation inhibitor cycloheximide (CHX) and either 5 μ M KHS101 or DMSO control. Cells were harvested at different times post-CHX treatment, and TACC3 protein levels were monitored by immunoblot (Figure 5a). KHS101 treatment decreased the stability of

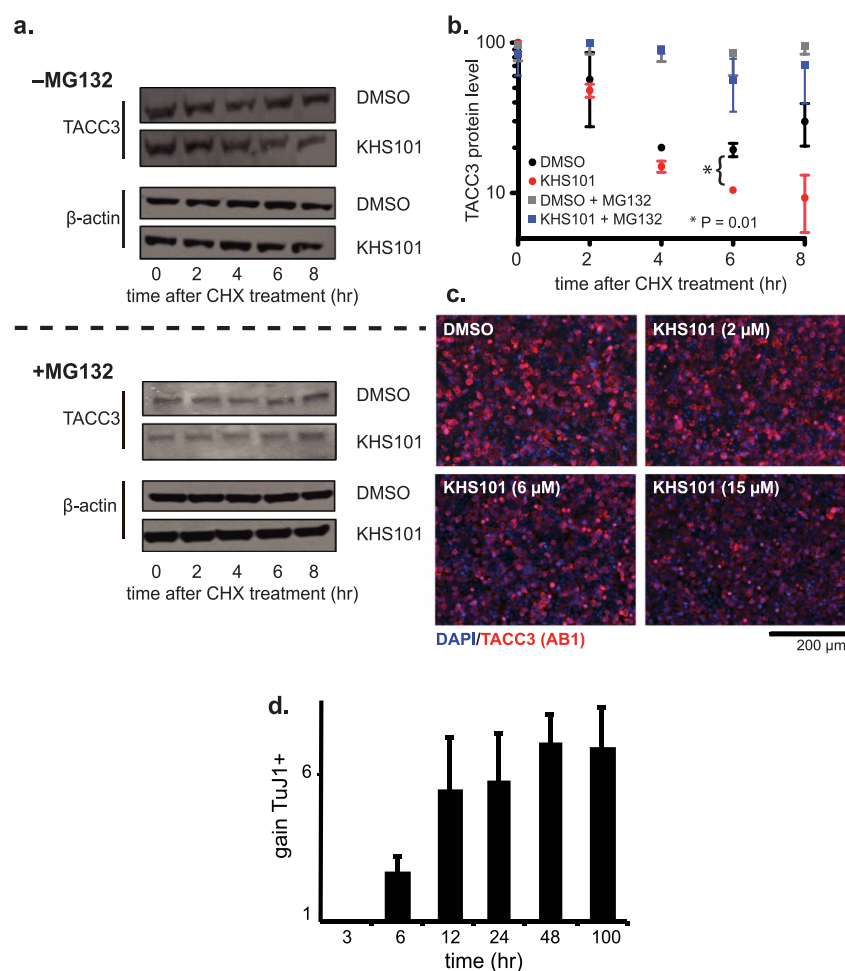


Figure 5. KHS101 decreases TACC3 levels in cells and regulates HIF gene expression. (a) KHS101 facilitates TACC3 degradation in a proteasome-dependent manner. HEK293T cells were treated with 5 μ M KHS101, 100 μ g/mL cycloheximide (CHX) (upper panel); additional cells were similarly treated with KHS101 and CHX plus 20 μ M MG132 (lower panel). Cells were harvested 0–8 h post-treatment and prepared for TACC3 immunoblot analyses. (b) Quantification of TACC3 protein levels from data shown in panel a. Without MG132, TACC3 protein levels decreased, with greater drops observed in KHS101-treated cells (compared to DMSO) after 6 h incubation. A statistically significant difference was observed 6 h post-treatment ($p < 0.01$ by Student's t test); the 8 h time point also shows a substantial decrease in TACC3 levels, but this is not statistically significant due to large variations in data values. In the presence of MG132, we observed little decrease in TACC3 levels with no KHS101-dependent effects, implicating a proteasome-dependent degradation pathway. (c) Steady state treatment with KHS101 reduces TACC3 levels. HEK293T cells were treated with KHS101 (0–15 μ M) and immunostained with TACC3 AB1 after 14 h. TACC3 intensity was negatively affected by KHS101. (d) KHS101 induces cell differentiation with a minimum of 6 h exposure. Adult rat NPCs were exposed to 5 μ M KHS101 (or DMSO) for the indicated times, after which media were replaced with compound-free versions and incubated for a total of 100 h. Neuronal differentiation was assessed by expression of the TuJ1 marker, showing upregulation after times consistent with TACC3 levels falling in CHX-treated cells (panels a and b).

TACC3 compared to DMSO controls (Figure 5a,b), with substantial differences after 6 h of treatment. We observe a statistically significant difference at 6 h and a net 3-fold drop in TACC3 protein levels at 8 h (relative levels of 9.3 [KHS101] and 29.9 [DMSO], Figure 5b), whereas ARNT levels were barely affected (Supplementary Figure S8a,b). In contrast, cells treated with KG-548 or an inactive KHS101 analogue, KHS91,²³ showed no change in TACC3 level compared with DMSO, indicating specificity in the ligand-induced degradation (Supplementary Figure S8c–g). Parallel experiments including the proteasome inhibitor MG132 muted this loss of TACC3 protein, without any marked difference between KHS101 and control groups (Figure 5a,b). Finally, we verified that KHS101 affects steady state TACC3 levels in the absence of CHX, showing a dose-dependent and saturable drop in TACC3 protein levels with increasing concentrations of KHS101 (Figure 5c, Supplementary Figure S9a–c). While this drop

was smaller than we observed with CHX treatment, the consistent observation of a 10% drop in TACC3 levels in independent experiments with different sample types (using either intact cells or cell lysates) and different primary antibodies (Supplementary Figure S9) gives us confidence in this trend. Taken together, our results suggest that KHS101 treatment leads to increased proteasome-mediated degradation of TACC3 protein in cells, conceivably mediated by interactions outside of the ARNT-binding motif.

KHS101 Treatment Affects Two Independent TACC3-Containing Pathways in Cells. To evaluate the functional implications of the KHS101-triggered drop in TACC3 levels, we looked for correlations between KHS101 effects on TACC3 levels and the activities of two TACC3-dependent pathways. We initially examined the kinetics of compound-induced NPC differentiation, which involves both TACC3 and ARNT2.²³ Here we used KHS101 washout experiments, exposing rat

NPCs to KHS101 for various times before switching to compound-free media for the remainder of the 100 h incubation. Afterward, differentiation was assessed using immunofluorescence-based detection of the pan-neuronal TuJ1 marker. We saw a KHS101-dependent increase in TuJ1 expression only after 6 h of treatment, maximizing after 12–24 h of exposure (Figure 5d). A reasonable hypothesis for this delay in KHS101 efficacy is that its proneurogenic effects are directly related to the time required to alter TACC3 protein levels (4–8 h by pulse chase; 16 h under steady state conditions).

To independently assess KHS101 effects in another TACC3-dependent activity, we examined the dose dependence of KHS101 on the transcription of endogenous HIF target genes using qPCR.¹⁴ Since KHS101 decreases steady state TACC3 levels, we suspected that compound treatment would lower TACC3 participation in hypoxia-induced HIF complexes, analogously to TACC3 knockdown and ARNT point mutations that weaken TACC3 binding.¹⁴ To test this possibility, we measured mRNA levels for three HIF-responsive genes in Hep3B cells, which utilize ARNT in both HIF-1 and HIF-2 signaling. Though some genes are regulated by both HIF paralogs, others are controlled only by either HIF-1 (e.g., PGK1) or HIF-2 (e.g., Epo).^{35,36} As expected, levels of these HIF-regulated transcripts increase (from 5- to 130-fold) upon exposure to hypoxia (Figure 6a). Concomitant treatment with KHS101 and hypoxia led to dose-dependent reductions in the levels of all three transcripts, with apparent IC₅₀ values below 5 μ M (Figure 6a), correlating the dose dependencies of KHS101 on TACC3 levels (Figure 5c). To further evaluate the mechanism of this effect, we quantitated HIF-1 α mRNA and protein levels by qPCR and Western blot. While HIF-1 α mRNA levels were unaffected by KHS101 treatment (Figure 6b), HIF-1 α protein levels were drastically decreased in a KHS101 dose-dependent manner (Figure 6c). We suspect HIF-2 α is similarly destabilized in KHS101-treated hypoxic cells, but quantitation of this effect is complicated by technical issues with available anti-HIF-2 α antibodies; compound treatment has no effect on HIF-2 α mRNA levels (data not shown). While further studies are needed to fully characterize the breadth of KHS101-induced protein destabilization with respect to several parameters (protein target, cell type, growth conditions), our functional data provide a mode of action for KHS101 and demonstrate its efficacy in two distinct pathways depending on cellular context.

DISCUSSION

Protein/protein interactions are often difficult to modulate with chemical reagents. Here we describe two compounds that affect the ARNT/TACC3 complex, an important component of HIF. These chemicals work by two different mechanisms: KG-548 directly interferes with ARNT/TACC3 complex formation by competing with TACC3 for binding to the ARNT PAS-B domain, while KHS101 modulates the abundance of both TACC3 and the HIF component, HIF-1 α . The different origins of these compounds underscore the merits of parallel *in vitro* target-based and cell-based phenotypic screens, each having strengths and weaknesses in drug discovery. *In vitro* target-based methods are appealing in their use of mechanism-driven hypotheses and focused searches for inhibitors of disease-associated targets, such as HIF or TACC3.^{37,38} However, this route often cannot address issues of potency, specificity, and metabolism that are essential for cellular applications, and

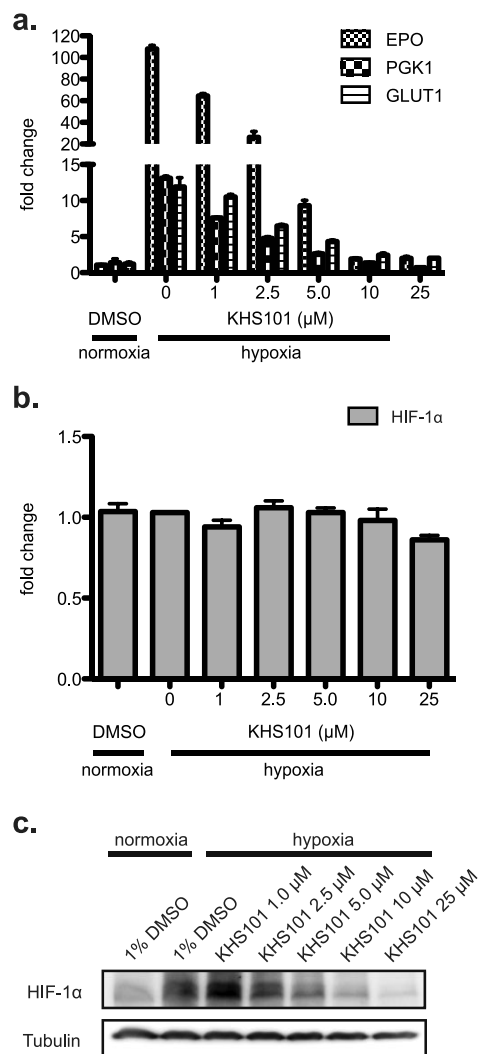


Figure 6. KHS101 inhibits HIF target gene expression and decreases HIF-1 α protein levels. (a) KHS101 treatment potently reduces HIF target gene expression. Hep3B cells were treated with KHS101 (0–25 μ M) and incubated under hypoxia (1% O₂) for 16 h. The expression of three HIF-driven genes (EPO, PGK1, GLUT1) were assessed by qPCR, demonstrating KHS101 inhibiting transcription with IC₅₀ < 5 μ M. (b) HIF-1 α mRNA level was measured by qPCR, showing no significant change with increasing KHS101 concentration. (c) HIF-1 α protein levels are reduced in a KHS101 dose-dependent manner, using anti-HIF-1 α Western blot.

which can be problematic to subsequently incorporate into lead compounds. In contrast, cell-based phenotypic methods have tremendous power to identify new inhibitors of biological activities but require downstream mechanistic studies to clarify modes of action. In our case, the linkage between ARNT2/TACC3 interactions and neuronal differentiation might have remained cryptic without the phenotypic screen and initial characterization of KHS101.^{22,23} While KHS101 demonstrates the potential of TACC3 destabilization to alter HIF transcriptional activation, we suggest that a target-based approach embodied by KG-548 can provide compounds that work more specifically than by simply destabilizing TACC3 and HIF-1 α , which may have potential secondary effects. Retrospective analyses of drug discovery successes underscore the utility of combining phenotypic and targeted approaches: the former still generate the majority of first-in-class new molecular entities but

are often followed by target-based screens which identify many more candidates using the foundation established by the phenotypic efforts.³⁹

From the standpoint of small molecule HIF inhibitors, blocking ARNT/TACC3 interactions may hold several advantages over previously described strategies.^{9,40–42} Most notably, this strategy targets a mechanistically defined interaction^{12,14} common among all three HIF paralogs, allowing a single compound to simultaneously block transcription from multiple HIFs given their shared use of ARNT. While our approach shares the general concept of disrupting activator/coactivator interactions with the HIF inhibitor chetomin,⁴¹ it is worth emphasizing that chetomin targets a completely different complex (HIF- α C-terminal transcriptional activation domain with the CH1 domain of the p300/CBP coactivator) that lacks the small-molecule binding pockets that confer specificity to ARNT PAS-B targeting compounds.

To close, integrating two screening strategies has provided us with small molecules that are useful tools for continuing studies of the critical HIF signaling pathway. This should also refine our understanding of the roles of CCC proteins in HIF-driven gene activation and could potentially lead to development of new therapeutic routes for HIF-dependent cancers. Finally, we hope that this parallel direct/indirect inhibitor approach provides another example in the relatively limited number of small molecule inhibitors of protein/protein interactions.

METHODS

Plasmids. For bacterial expression, human ARNT (356–470) and ARNT2 PAS-B domain (330–444) constructs were cloned into pHis-Parallel,⁴³ while murine TACC3 constructs (TACC3-CT=561–631; GCN4-TACC3-min=GCN4 coiled coil + residues 610–631) were cloned into pGST- and pHis-Parallel, respectively.⁴³ Full-length human ARNT and murine TACC3 were cloned into pcDNA4B vector (Invitrogen) with a C-terminal FLAG (ARNT) or myc-His₆ (TACC3) tags for mammalian cell transfection.

Compound Sources. KHS101 was kindly provided by Dr. Peter Schultz (The Scripps Research Institute), synthesized as described.²³ KG-548 was purchased from Fluorochem and resupplied from Matrix Scientific; the composition of the entire fragment-based library is detailed in Supporting Table S1.

Immunoblot, Pulldown, and Immunofluorescence Assays. For immunoblots, proteins resolved from SDS-PAGE gels were transferred to PVDF membranes (GE Healthcare) and immunoblotted with these antibodies: anti-ARNT (A-3), anti-TACC3 (T-17), anti-goat IgG-HRP (Santa Cruz Biotechnology); anti-TACC3 (ab56595) (abcam); anti-Myc (9E10), anti-HIF1 α (BD Transduction Laboratories); anti-mouse IgG-HRP antibodies (Sigma). For pulldown experiments, 5 μ M purified His-ARNT/ARNT2 PAS-B and 8–15 μ M TACC3-CT were incubated with 15 μ L of Ni-NTA beads overnight at 4 °C. Eluted protein was resolved in SDS-PAGE and stained with Coomassie Blue stain. Immunofluorescence studies of steady state TACC3 levels used HEK293 cells stained with an anti-TACC3 rabbit polyclonal antibody (Sigma-Aldrich HPA005781; here called TACC3 AB1); more details are provided in Supporting Information.

Protein Expression and Purification. Proteins were expressed in BL21(DE3) cells and purified using standard FPLC-based methods (detailed in Supporting Information).

Structural Studies. Structural studies of ARNT PAS-B were conducted using standard crystallization and X-ray diffraction methods, detailed in Supporting Information. Coordinates of the resulting structure have been deposited in the RCSB (accession code 4EQ1), with refinement information in Table 1. Solution NMR studies of ARNT2 PAS-B utilized U-¹⁵N,¹³C labeled proteins and triple resonance assignment methods, also detailed in Supporting Information.

AlphaScreen Assay. 400 nM His-ARNT PAS-B and 400 nM GST-TACC3-CT E629A were mixed in a 384-well plate with a total volume of 15 μ L and incubated at 4 °C for 1 h. AlphaScreen glutathione donor beads and AlphaLISA Ni chelate acceptor beads (5 μ g/mL each; Perkin-Elmer) were added under dim green light in 50 mM Tris (pH 7.5), 100 mM NaCl, 0.02% Tween 20, and 1 mM DTT. After incubating in a dark and humidified chamber for 3.5 h, the plate was read using an Envision plate reader (Perkin-Elmer).

KHS101 Washout Assay. Adult rat hippocampal NPCs were differentiated upon treatment with 5 μ M KHS101 or a DMSO negative control as previously described.²³ After incubation for times shown in Figure 5d, the culture medium was replaced with fresh (compound-free) media. After a total 100 h incubation period, cells were fixed and stained for the neuronal marker TuJ1.²³ Neuronal differentiation of KHS101-treated rat hippocampal NPCs was analyzed by microscopy, the percentage of TuJ1-positive cells was determined, and data were normalized to the DMSO control values.

TACC3 Turnover Assay. HEK293T cells were treated with 5 μ M KHS101 and 100 μ g/mL cycloheximide (CHX) with or without 20 μ M MG132. DMSO treatment served as a negative control. Cells were harvested at several time points from 0 to 8 h post-treatment and prepared for TACC3, ARNT and β -actin immunoblot analyses.

qPCR. Cells were collected with Trizol (Invitrogen), and total RNA was extracted using the RNeasy Mini Kit (Qiagen). Following DNase treatment, cDNA was synthesized from 1 μ g of RNA using SuperScript II Reverse Transcriptase (Invitrogen) in final volume of 50 μ L. Real-time PCR was performed (with target gene primers listed in Supporting Information) on 1.25 μ L of cDNA in triplicate using Power SYBR Green PCR Master Mix and the 7900HT Fast Real-Time PCR System (Applied Biosystems). Target gene expression levels were normalized to the expression level of cyclophilin B in the same sample. Data were analyzed using the comparative C_T method ($2^{-\Delta\Delta C_T}$)⁴⁴ and normalized to normoxia/1% DMSO conditions.

ASSOCIATED CONTENT

Supporting Information

Detailed experimental procedures, supplementary figures, and supplementary table. This material is available free of charge via the Internet at <http://pubs.acs.org>.

AUTHOR INFORMATION

Corresponding Author

*E-mail: kevin.gardner@utsouthwestern.edu.

Present Address

^{||}Chemistry and Biochemistry Department, UC Santa Cruz, 1156 High St., Santa Cruz, CA 95064.

Author Contributions

Y.G., C.L.P., J.K., P.B.C., V.P., R.K.B., H.W., and K.H.G. designed research; Y.G., C.L.P., J.K., P.B.C., V.P., A.P. and H.W. performed research; Y.G., C.L.P., J.K., P.B.C., V.P., R.K.B., H.W. and K.H.G. analyzed data; Y.G., C.L.P., J.K., P.B.C., R.K.B., H.W. and K.H.G. wrote the paper.

Notes

The authors declare no competing financial interests.

ACKNOWLEDGMENTS

This work was supported by grants from the NIH (R01 GM081875 to K.H.G.; P01 CA095471 and R21 NS067624 to K.H.G. and R.K.B.; F32 CA130441 to C.L.P.), CPRIT (RP100846 to K.H.G. and R.K.B.), and the Burroughs Wellcome Fund (R.K.B.). KHS101 was kindly provided as a gift from P. Schultz (The Scripps Research Institute, La Jolla, CA). Portions of this work were conducted in facilities constructed with support from the Research Facilities Improve-

ment Program (Grant no. C06 RR 15437-01) from the NIH/National Center for Research Resources or at Argonne National Laboratory, Structural Biology Center at the Advanced Photon Source, supported by U.S. Department of Energy, Office of Biological and Environmental Research Contract DE-AC02-06CH11357.

REFERENCES

- (1) Koehler, A. N. (2010) A complex task? Direct modulation of transcription factors with small molecules. *Curr. Opin. Chem. Biol.* 14, 331–340.
- (2) Wells, J. A., and McClendon, C. L. (2007) Reaching for high-hanging fruit in drug discovery at protein-protein interfaces. *Nature* 450, 1001–1009.
- (3) Darnell, J. E., Jr. (2002) Transcription factors as targets for cancer therapy. *Nat. Rev. Cancer* 2, 740–749.
- (4) Majumdar, A. J., Wong, W. J., and Simon, M. C. (2010) Hypoxia-inducible factors and the response to hypoxic stress. *Mol. Cell* 40, 294–309.
- (5) Semenza, G. L. (2012) Hypoxia-inducible factors in physiology and medicine. *Cell* 148, 399–408.
- (6) Gordan, J. D., and Simon, M. C. (2007) Hypoxia-inducible factors: central regulators of the tumor phenotype. *Curr. Opin. Genet. Dev.* 17, 71–77.
- (7) Erbel, P. J., Card, P. B., Karakuzu, O., Bruick, R. K., and Gardner, K. H. (2003) Structural basis for PAS domain heterodimerization in the basic helix–loop–helix-PAS transcription factor hypoxia-inducible factor. *Proc. Natl. Acad. Sci. U.S.A.* 100, 15504–15509.
- (8) Yang, J., Zhang, L., Erbel, P. J. A., Gardner, K. H., Ding, K. M., Garcia, J. A., and Bruick, R. K. (2005) Functions of the Per/ARNT/Sim (PAS) domains of the hypoxia inducible factor (HIF). *J. Biol. Chem.* 280, 36047–36054.
- (9) Scheuermann, T. H., Tomchick, D. R., Machius, M., Guo, Y., Bruick, R. K., and Gardner, K. H. (2009) Artificial ligand binding within the HIF2 α PAS-B domain of the HIF2 transcription factor. *Proc. Natl. Acad. Sci. U.S.A.* 106, 450–455.
- (10) Key, J., Scheuermann, T. H., Anderson, P. C., Daggett, V., and Gardner, K. H. (2009) Principles of ligand binding within a completely buried cavity in HIF2 α PAS-B. *J. Am. Chem. Soc.* 131, 17647–17654.
- (11) Hao, N., Whitelaw, M. L., Shearwin, K. E., Dodd, I. B., and Chapman-Smith, A. (2011) Identification of residues in the N-terminal PAS domains important for dimerization of Arnt and AhR. *Nucleic Acids Res.* 39, 3695–3709.
- (12) Partch, C. L., Card, P. B., Amezcua, C. A., and Gardner, K. H. (2009) Molecular basis of coiled coil coactivator recruitment by the aryl hydrocarbon receptor nuclear translocator (ARNT). *J. Biol. Chem.* 284, 15184–15192.
- (13) Partch, C. L., and Gardner, K. H. (2010) Coactivator recruitment: a new role for PAS domains in transcriptional regulation by the bHLH-PAS family. *J. Cell. Physiol.* 223, 553–557.
- (14) Partch, C. L., and Gardner, K. H. (2011) Coactivators necessary for transcriptional output of the hypoxia inducible factor, HIF, are directly recruited by ARNT PAS-B. *Proc. Natl. Acad. Sci. U.S.A.* 108, 7739–7744.
- (15) Beischlag, T. V., Taylor, R. T., Rose, D. W., Yoon, D., Chen, Y., Lee, W. H., Rosenfeld, M. G., and Hankinson, O. (2004) Recruitment of thyroid hormone receptor/retinoblastoma-interacting protein 230 by the aryl hydrocarbon receptor nuclear translocator is required for the transcriptional response to both dioxin and hypoxia. *J. Biol. Chem.* 279, 54620–54628.
- (16) Kim, J. H., and Stallcup, M. R. (2004) Role of the coiled-coil coactivator (CoCoA) in aryl hydrocarbon receptor-mediated transcription. *J. Biol. Chem.* 279, 49842–49848.
- (17) Sadek, C. M., Jalaguier, S., Feeney, E. P., Aitola, M., Damdimopoulos, A. E., Pelto-Huikko, M., and Gustafsson, J. A. (2000) Isolation and characterization of AINT: a novel ARNT interacting protein expressed during murine embryonic development. *Mech. Dev.* 97, 13–26.
- (18) Henry, J. T., and Crosson, S. (2011) Ligand-binding PAS domains in a genomic, cellular, and structural context. *Annu. Rev. Microbiol.* 65, 261–286.
- (19) Card, P. B., Erbel, P. J. A., and Gardner, K. H. (2005) Structural basis of ARNT PAS-B dimerization: Use of a common beta-sheet interface for hetero- and homodimerization. *J. Mol. Biol.* 353, 664–677.
- (20) Amezcua, C. A., Harper, S. M., Rutter, J., and Gardner, K. H. (2002) Structure and interactions of PAS kinase N-terminal PAS domain: model for intramolecular kinase regulation. *Structure* 10, 1349–1361.
- (21) Best, J. L., Amezcua, C. A., Mayr, B., Flechner, L., Murawsky, C. M., Emerson, B., Zor, T., Gardner, K. H., and Montminy, M. (2004) Identification of small-molecule antagonists that inhibit an activator: coactivator interaction. *Proc. Natl. Acad. Sci. U.S.A.* 101, 17622–17627.
- (22) Warashina, M., Min, K. H., Kuwabara, T., Huynh, A., Gage, F. H., Schultz, P. G., and Ding, S. (2006) A synthetic small molecule that induces neuronal differentiation of adult hippocampal neural progenitor cells. *Angew. Chem., Int. Ed.* 45, 591–593.
- (23) Wurdak, H., Zhu, S., Min, K. H., Aimone, L., Lairson, L. L., Watson, J., Chopiuk, G., Demas, J., Charette, B., Halder, R., Weerapana, E., Cravatt, B. F., Cline, H. T., Peters, E. C., Zhang, J., Walker, J. R., Wu, C., Chang, J., Tuntland, T., Cho, C. Y., and Schultz, P. G. (2010) A small molecule accelerates neuronal differentiation in the adult rat. *Proc. Natl. Acad. Sci. U.S.A.* 107, 16542–16547.
- (24) Crosson, S., and Moffat, K. (2001) Structure of a flavin-binding plant photoreceptor domain: Insights into light-mediated signal transduction. *Proc. Natl. Acad. Sci. U.S.A.* 98, 2995–3000.
- (25) Gong, W., Hao, B., Mansy, S. S., Gonzalez, G., Gilles-Gonzalez, M. A., and Chan, M. K. (1998) Structure of a biological oxygen sensor: a new mechanism for heme-driven signal transduction. *Proc. Natl. Acad. Sci. U.S.A.* 95, 15177–15182.
- (26) Genick, U. K., Borgstahl, G. E., Ng, K., Ren, Z., Pradervand, C., Burke, P. M., Srajer, V., Teng, T. Y., Schildkamp, W., McRee, D. E., Moffat, K., and Getzoff, E. D. (1997) Structure of a protein photocycle intermediate by millisecond time-resolved crystallography. *Science* 275, 1471–1475.
- (27) Hajduk, P. J., Bures, M., Praestgaard, J., and Fesik, S. W. (2000) Privileged molecules for protein binding identified from NMR-based screening. *J. Med. Chem.* 43, 3443–3447.
- (28) Moglich, A., Ayers, R. A., and Moffat, K. (2009) Structure and signaling mechanism of Per-ARNT-Sim domains. *Structure* 17, 1282–1294.
- (29) Hirose, K., Morita, M., Ema, M., Mimura, J., Hamada, H., Fujii, H., Saijo, Y., Gotoh, O., Sogawa, K., and Fujii-Kuriyama, Y. (1996) cDNA cloning and tissue-specific expression of a novel basic helix-loop-helix/PAS factor (Arnt2) with close sequence similarity to the aryl hydrocarbon receptor nuclear translocator (Arnt). *Mol. Cell. Biol.* 16, 1706–1713.
- (30) Sekine, H., Mimura, J., Yamamoto, M., and Fujii-Kuriyama, Y. (2006) Unique and overlapping transcriptional roles of arylhydrocarbon receptor nuclear translocator (Arnt) and Arnt2 in xenobiotic and hypoxic responses. *J. Biol. Chem.* 281, 37507–37516.
- (31) Shen, Y., Delaglio, F., Cornilescu, G., and Bax, A. (2009) TALOS+: a hybrid method for predicting protein backbone torsion angles from NMR chemical shifts. *J. Biomol. NMR* 44, 213–223.
- (32) Huang, N., Chelliah, Y., Shan, Y., Taylor, C. A., Yoo, S. H., Partch, C., Green, C. B., Zhang, H., and Takahashi, J. S. (2012) Crystal structure of the heterodimeric CLOCK:BMAL1 transcriptional activator complex. *Science* 337, 189–194.
- (33) Barelier, S., and Krimm, I. (2011) Ligand specificity, privileged substructures and protein druggability from fragment-based screening. *Curr. Opin. Chem. Biol.* 15, 469–474.
- (34) Cappell, K. M., Sinnott, R., Taus, P., Maxfield, K., Scarbrough, M., and Whitehurst, A. W. (2012) Multiple cancer testis antigens function to support tumor cell mitotic fidelity. *Mol. Cell. Biol.* 32, 4131–4140.

(35) Dioum, E. M., Chen, R., Alexander, M. S., Zhang, Q., Hogg, R. T., Gerard, R. D., and Garcia, J. A. (2009) Regulation of hypoxia-inducible factor 2 α signaling by the stress-responsive deacetylase sirtuin 1. *Science* 324, 1289–1293.

(36) Scortegagna, M., Ding, K., Zhang, Q., Oktay, Y., Bennett, M. J., Bennett, M., Shelton, J. M., Richardson, J. A., Moe, O., and Garcia, J. A. (2005) HIF-2 α regulates murine hematopoietic development in an erythropoietin-dependent manner. *Blood* 105, 3133–3140.

(37) Qing, G., and Simon, M. C. (2009) Hypoxia inducible factor-2 α : a critical mediator of aggressive tumor phenotypes. *Curr. Opin. Genet. Dev.* 19, 60–66.

(38) Lauffart, B., Vaughan, M. M., Eddy, R., Chervinsky, D., DiCioccio, R. A., Black, J. D., and Still, I. H. (2005) Aberrations of TACC1 and TACC3 are associated with ovarian cancer. *BMC Womens Health* 5, 8.

(39) Swinney, D. C., and Anthony, J. (2011) How were new medicines discovered? *Nat. Rev. Drug Discovery* 10, 507–519.

(40) Park, E. J., Kong, D., Fisher, R., Cardellina, J., Shoemaker, R. H., and Melillo, G. (2006) Targeting the PAS-A domain of HIF-1 α for development of small molecule inhibitors of HIF-1. *Cell Cycle* 5, 1847–1853.

(41) Kung, A. L., Zabudoff, S. D., France, D. S., Freedman, S. J., Tanner, E. A., Vieira, A., Cornell-Kennon, S., Lee, J., Wang, B., Wang, J., Memmert, K., Naegeli, H. U., Petersen, F., Eck, M. J., Bair, K. W., Wood, A. W., and Livingston, D. M. (2004) Small molecule blockade of transcriptional coactivation of the hypoxia-inducible factor pathway. *Cancer cell* 6, 33–43.

(42) Lee, K., Zhang, H., Qian, D. Z., Rey, S., Liu, J. O., and Semenza, G. L. (2009) Acriflavine inhibits HIF-1 dimerization, tumor growth, and vascularization. *Proc. Natl. Acad. Sci. U.S.A.* 106, 17910–17915.

(43) Sheffield, P., Garrard, S., and Derewenda, Z. (1999) Overcoming expression and purification problems of RhoGDI using a family of "parallel" expression vectors. *Protein Expression Purif.* 15, 34–39.

(44) Bookout, A. L., and Mangelsdorf, D. J. (2003) Quantitative real-time PCR protocol for analysis of nuclear receptor signaling pathways. *Nucl. Recept. Signaling* 1, e012.

(45) Farmer, B. T., Constantine, K. L., Goldfarb, V., Friedrichs, M. S., Wittekind, M. G., Yanchunas, J. J., Robertson, J. G., and Mueller, L. (1996) Localizing the NADP⁺ binding site on the MurB enzyme by NMR. *Nat. Struct. Biol.* 3, 995–997.